Unusual Viral Ligand With Alternative Interactions Is Presented by HLA-Cw4 in Human Respiratory Syncytial Virus-Infected Cells

Susana Infantes, Elena Lorente, Juan José Cragnolini, Manuel Ramos, Ruth García, Mercedes Jiménez, Salvador Iborra, Margarita Del Val, Daniel López

Immunol Cell Biol. 2011 May;89(4):558-65.

https://doi.org/10.1038/icb.2010.125

UNUSUAL VIRAL LIGAND WITH ALTERNATIVE INTERACTIONS IS PRESENTED BY HLA-Cw4 IN HUMAN RESPIRATORY SYNCYTIAL VIRUS-INFECTED CELLS

Susana Infantes [1], Elena Lorente [1], Juan José Cragnolini [2], Manuel Ramos [3], Ruth García [1], Mercedes Jiménez [4], Salvador Iborra [3], Margarita Del Val [2,3], Daniel López [1,4,*]

[1] Unidad de Procesamiento Antigénico, [3] Unidad de Inmunología Viral, and [4] Unidad de Proteómica and Centro Nacional de Microbiología. Instituto de Salud Carlos III. 28220 Majadahonda (Madrid), Spain.

[2] Centro de Biología Molecular Severo Ochoa, CSIC/Universidad Autónoma de Madrid, 28049 Madrid, Spain.

Short Running Title: Natural HLA-Cw4 ligand without anchor motifs

* Correspondence to: Dr. Daniel López. Unidad de Proteómica. Centro Nacional de Microbiología. Instituto de Salud Carlos III. 28220 Majadahonda (Madrid), Spain. Tel: +34 91 822 37 08, FAX: +34 91 509 79 19, E-mail address: dlopez@isciii.es.

ABSTRACT

Short viral antigens bound to human major histocompatibility complex (HLA) class I molecules are presented on infected cells. Vaccine development frequently relies on synthetic peptides to identify optimal HLA class I ligands. However, when natural peptides are analyzed, more complex mixtures are found. By immunoproteomics analysis, we identify here a physiologically processed HLA ligand derived from human respiratory syncytial virus matrix protein that is very different from what was expected from studies with synthetic peptides. This natural HLA-Cw4 class I ligand uses alternative interactions to the anchor motifs previously described for its presenting HLA-Cw4 class I molecule. Finally, this octameric peptide shares its C-terminal core with the H-2D^{b} nonamer ligand previously identified in the mouse model. These data have implications for the identification of antiviral CTL responses and for vaccine development.

Keywords: antigen processing, mass spectrometry, MHC class I, virus, vaccine.

INTRODUCTION

Proteolytic degradation of newly synthesized viral proteins in the cytosol by the combined action of proteasomes and degradative peptidases is the first step in the recognition of virus-infected cells by cytotoxic T lymphocytes (CTL) [1]. This processing generates peptides of 8 to 10 residues that are translocated to the endoplasmic reticulum lumen by transporters associated with antigen processing, and these short peptides assemble with human histocompatibility complex (HLA) class I heavy chain and β_2-microglobulin. Typically, this interaction is made possible by two major anchor residues at position 2 and the C-terminus of the antigenic peptide [2,3] that are deeply accommodated into specific pockets of the antigen recognition site of the HLA class I molecule [4,5]. Finally, the stable trimolecular peptide-HLA-β_2-microglobulin complexes are transported to the cell membrane and presented for CTL recognition [6].

Human respiratory syncytial virus (HRSV) [7], a *Pneumovirus* of the *Paramyxoviridae* family is an enveloped virus containing a negative-sense, single-stranded RNA genome encoding 11 proteins. This virus is the single most important cause of serious lower respiratory tract illnesses such as bronchiolitis and pneumonia in infants and young children [8-10]. HRSV also infects people of all ages but mainly poses a serious health risk in immunocompromised individuals [11,12] and in the elderly [13,14]. Although the immune mechanisms involved in HRSV disease and protection are not fully understood the $CD8^+$ T lymphocytes are required to clear virus-infected cells [15]. In recent years, several HRSV epitopes restricted by different HLA class I molecules have been identified using the CTL of seropositive individuals [16-20]. However, all these experiments were performed with synthetic peptides and no identification of natural epitopes was performed. Two previous studies on the identification of the natural peptides that are endogenously processed in living cells from the HIV gp160 glycoprotein and then presented by murine MHC class I molecules showed multiple additional ligands differing from the optimal antigenic synthetic peptide [21,22]. Thus, further studies on the

natural peptides involved in the antiviral CTL response are needed. To date, only two naturally processed HRSV ligands have been reported [23]. We are interested in extending the study of the natural peptides responsible for the HRSV antiviral response. By means of a comparative immunoproteomics analysis of peptide pools isolated from uninfected and virus-infected cells, this report identifies an unusual HLA ligand different from that predicted by bioinformatics tools. These results underscore the need to study the peptides produced by physiological processing, as the natural situation may be different from the one defined with synthetic peptides.

RESULTS

Identification of endogenously processed HLA ligands derived from HRSV in infected human cells.

The strategy used in this study was adapted from the identification of HLA-B27-ligands from stable transfectants expressing individual bacterial proteins as previously reported [24,25]. First, HLA-bound peptide repertoires were isolated from cells either infected or not infected with HRSV. Next, both peptide pools were fractionated by HPLC in consecutive runs and under identical conditions to reduce alterations in the peptide elution patterns. Analysis of every HPLC fraction from each peptide pool was done by MALDI-TOF MS. Each spectrum of a single HPLC fraction of HRSV-infected cells was compared manually with the correlative (i), two previous (i-1, and i-2) and two following (i+1, and i+2) fractions of the uninfected cells. This technique allows the selection of peptides found only in the HRSV-infected cells. The corresponding MS/MS spectrum of each differential peptide was obtained and its amino acid sequence was assigned with bioinformatics tools. The sequences were validated by comparison with the MS/MS spectrum of the corresponding synthetic peptide.

A single viral HLA ligand differentially detected in HRSV-infected cells.

B27-C1R transfected cells were used as starting point because they express high levels of HLA-B27 and minimal levels of other HLA class I molecules. B27-C1R cells were incubated with the Long strain of HRSV and assayed at different times for the presence of HRSV antigens by flow cytometry. The results shown in Figure 1 indicate that after two weeks the transfectant cell line incubated with the virus, but not the mock infected control, was expressing HRSV F and/or G proteins. Similar results were obtained at longer time periods post-infection (data not shown). Thus, a B27-C1R

transfectant cell line persistently infected with HRSV was obtained in the same manner as previously reported for Epstein-Barr-transformed human B-cell lines [26]. HLA-bound peptide pools were then isolated from B27-C1R cells and HRSV-infected B27-C1R cells. Next, a comparative analysis of MALDI-TOF MS was carried out. Twenty-two ion peaks that were detected in different HPLC fractions of the $HRSV^+$ cell line but not in the uninfected controls were analyzed by ESI-IT MS/MS (data not shown). Only one ion peak with an m/z of 422.9 was assigned to the viral amino acid sequence AITNAKII, spanning residues 188-195 of the HRSV matrix protein (Fig. 2, upper panel). A search in the human proteome database failed to identify any human protein, confirming the viral origin of this peptide. The theoretical assignment was confirmed by identity with the MS/MS spectrum of the corresponding synthetic peptide (Fig. 2, lower panel). Thus, these results indicate that an HRSV ligand is endogenously processed and presented by an HLA molecule of the B27-C1R cell line.

HRSV M188-195 is a non canonical HLA-Cw4 ligand.

Following a similar strategy to the one used in this study, in recent years several hundred HLA-B27 ligands have been identified by immunoprecipitation with the W6/32 mAb of HLA-B27-peptide complexes using the B27-C1R cell line (summarized in the SYFPEITHI database: http://www.syfpeithi.de [3]). This MHC class I molecule binds peptides with Arg at position 2 and basic, aliphatic or aromatic C-terminal residues [27]. The HRSV matrix 188-195 ligand AITNAKII identified in Figure 1 does not have the canonical HLA-B27 anchor motifs. One possibility is that it could be an unusual HLA-B27-restricted ligand. To test this hypothesis, MHC/peptide complex stability assays were carried out using TAP-deficient RMA-S cells transfected with HLA-B27. Figure 3a shows that in contrast to a control HLA-B27 viral ligand, the influenza virus NP peptide, induction of complexes with the HRSV matrix 188-195 peptide was not detected. Thus, this viral ligand does not bind to HLA-B27.

The C1R cell line has been widely used as a transfection recipient in functional studies of MHC class I genes because it barely expresses HLA-A and –B molecules, as it is derived from a normal EBV-transformed B cell line modified by several rounds of mutagenesis and immunoselection with anti-HLA antibodies and complement [28]. A later study [29] demonstrated that, in this heterozygous cell line, the chromosomic region encoding HLA-A3, Bw62, and Cw3 class I molecules is deleted; meanwhile, the expression of HLA-B35 and –Cw4 is weakly positive and the expression of HLA-A2 appears to be negative [29]. Thus, new MHC/peptide complex stability assays using TAP-deficient RMA-S cells transfected with each HLA molecule of the C1R cell line were performed. No HLA stabilization was detected using either HLA-$A2^+$ (Fig. 3b) or –$B35^+$ (Fig. 3c) cells. These data indicate that the AITNAKII peptide is not restricted by these HLA molecules. In contrast, the M188-195 synthetic peptide induced similar numbers of HLA-peptide surface complexes as a well-known HLA-Cw4 ligand, C4CON (Fig. 4, upper left panel). The consensus peptide binding motif for HLA-Cw4 is Tyr or Phe at peptide position 2 [30,31]. Thus, the M188-195 octamer is an unusual HLA-Cw4 ligand.

Identical binding hierarchy to human and mouse MHC class I molecules in two nested viral peptides.

Interestingly, the M187-195 NAITNAKII nonamer has been described as an H-$2D^b$-restricted CTL epitope [32] and it has the canonical anchor motifs for D^b molecules [33]. Therefore, two viral peptide species of different lengths that share the same antigenic core and differ only in the additional N-terminal residue were bound to either HLA-Cw4 or H-$2D^b$ presenting molecules in the respective infected cells. Next, binding of the AITNAKII octamer and the related nonamer was tested in these two MHC class I molecules. The results indicate that both peptides stabilize significant surface MHC-peptide complexes in HLA-Cw4 (Fig. 4, upper left panel) or H-$2D^b$ (Fig. 4, upper right

panel) positive cells. In addition, the relative MHC class I affinity of both peptides was evaluated. Both peptides bound to MHC class I molecules in the range commonly found among natural ligands (Fig. 5). The nonamer efficiently stabilized HLA-Cw4 (Fig. 5, left panel) and H-2D^b (Fig. 5, right panel) cells, with a C_{50} for MHC binding of 1.5 ± 1 µM and 2 ± 1 µM respectively. MHC class I molecules on both cell lines were stabilized about 10-fold less efficiently with the octamer (Fig. 5) but still in the range of optimal ligands. Surprisingly, both the octamer and the nonamer bound efficiently to HLA-Cw4 molecules, in spite of the lack of canonical anchors for interaction with the presenting molecule.

In summary, the two peptides show identical binding patterns in both human and mouse cells.

Differential conformation of HRSV octamer and nonamer peptides bound to the HLA-Cw4 molecule.

Only one crystal structure of HLA-Cw4, in complex with the peptide QYDDAVYKL, has been described [34]. This C4CON peptide is anchored to four specificity pockets in the binding groove. The A pocket interacts with both the terminal NH_2 and the side chain of the P1 Gln residue (Fig. 6a). The B pocket interacts with the P2 Tyr residue. HLA-Cw4 presents an E pocket located on the side of the α1 helix, formed mostly by residues from the α1 helix and the β sheet platform that bind the P7 Tyr side chain of the peptide. Last, the F pocket forms the COOH-terminal boundary of the cleft and is incompletely filled by the side chain of P9 Leu. Modeling of both HRSV nonamer and octamer peptides in complex with HLA-Cw4 was performed on the basis of the existing X-ray structure of the QYDDAVYKL-HLA-Cw4 complex (Fig. 6a). The CΩ Ile residue of both peptides interacted with the C-terminal F pocket as did the P9 Leu of the QYDDAVYKL peptide (Fig. 6b and c). In the HRSV nonamer, P3 Ile and P7 Lys must be accommodated into the B and E pockets, respectively, with residues 4-6

and 8 bulging out of the peptide binding cleft (Figure 6b). In this HRSV nonamer, the existence of P1 Asn allows recovery of the interaction of the amide group of P1 Gln with the HLA-Cw4 molecule shown by the crystallographic data (Figure 6a and b). The shorter lateral chain of Asn versus Gln allows inclusion of the small Ala residue in the P2 position with little variation in peptide conformation. In contrast, in the octamer the P1 Ala terminal NH_2 group interacts identically to the equivalent groups of either Gln of QYDDAVYKL or Asn of the nonamer peptide. The interactions of the terminal NH_2 group and the lateral chain of CΩ with the HLA molecule stretch the octameric peptide and thus either P2 Ile or P6 Lys cannot be accommodated as in the nonameric peptide. These losses in interaction of the 8mer to HLA may explain the differences between the octamer and the nonamer detected in the MHC stabilization assay (Fig. 5).

To demonstrate that the 8mer and 9mer viral peptides are bound with different register to HLA-Cw4 molecules, new MHC/peptide complex stability assays with monosubstituted Ala analogues of HRSV Matrix peptides were carried out. The exchange for Ala of the Ile residue that serves as anchor motif, but not the P3 Thr that is solvent exposed, abolished the interaction with the MHC of the octamer (Fig. 7, left panel) but not with the nonamer (Fig. 7, right panel). The additional anchor interactions with HLA molecule of P1 Asn, and P7 Lys in the 9mer, that were absent in the octamer as suggest the modeling of Figure 6, could compensate the loss of P3 Ile by Ala exchange and explain the stabilization of the A3-9 (Ala → Ile) 9mer.

DISCUSSION

The results reported here show that the octamer 188-195 derived from the HRSV matrix protein is efficiently processed in HRSV infected cells. This ligand is presented by the MHC class I molecule Cw4 using alternative interactions to the anchor motifs previously described for this MHC class I molecule. In addition, this octameric peptide coincides with the C-terminal core of a putative H-2D^{b}-restricted CTL nonameric epitope previously identified in the mouse model.

In a previous study that involved culturing virus-infected cells with stable isotope-labeled amino acids expected to be anchor residues for the HLA allele of interest and then performing immunoprecipitation of MHC molecules and two-dimensional nanoscale LC-MS analysis, one HRSV ligand for each HLA-A2 or –B7 class I molecule was identified [23]. In our current study, which uses similar cell numbers and a more classical and cheaper approach, one HRSV HLA ligand was also identified. Isotope labeling of anchor residues strongly favors detection of peptides with the canonical anchors. Thus, artificial biases are introduced when using such a directed methodology in these difficult studies, and unusual viral ligands such as M188-195 may pass undetected. In addition, the identification of one viral ligand per heterozygous HLA-A, -B and -C cell line in both previous [23] and current studies of HRSV infected cells could indicate immunodominant selection of ligands or only low coverage of identified peptides. Thus, future studies using new high resolution mass spectrometers are needed to clarify this point.

Furthermore, our detection of an endogenously presented natural viral peptide without the HLA-Cw4 anchor motifs reveals the limitations of predictive methods for identifying natural MHC class I ligands and T-cell epitopes. These analytical algorithms may not be sufficiently accurate and their cautious use is highly recommended. Currently, about fifty endogenously processed HLA-Cw4 ligands derived from cellular proteins have been identified with Tyr or Phe at peptide position 2 as anchor motif [30,31].

In contrast, there are very few studies identifying viral HLA-Cw4 ligands or CTL epitopes. The peptide NVFPIFLQM spanning residues 54-62 of the human papillomavirus 18 L1 protein was eluted from purified HLA-Cw4 molecules [35]. This viral peptide, with N-terminal Asn followed by a relatively small residue in the P2 position, resembles nonameric D^b ligand NAITNAKII derived from HRSV matrix protein, which also binds to Cw4 as a synthetic peptide. Probably, the first 3 residues of both nonameric viral peptides bind similarly to HLA-Cw4, with the hydrophobic residues in position 3 occupying the B pocket of the HLA molecule as suggested by our modelling (Fig. 6). In addition, two HIV HLA-Cw4-restricted epitopes have previously been reported in gp120 (FNCGGEFF, residues 377-383) [36] and in the protease (QYDQIPIEI, residues 58-66) [37]. As the novel viral ligand AITNAKII found in our current study, two of these three ligands did not show the consensus peptide motif for binding to HLA-Cw4. Thus, the use of predictive algorithms based on parameters such as MHC class I binding motifs for identifying natural viral HLA class I ligands and T-cell epitopes may not be pertinent for some MHC class I molecules, such as HLA-Cw4.

Our study also reveals that the natural 8mer presented by HLA-Cw4 almost coincides with a published 9mer presented by murine D^b class I molecule. Past studies have shown interspecies cross-reactivity of MHC class I epitopes. These included 5, 3, and 1 ligands shared by a human and a rhesus macaque, a rhesus macaque and a mouse, and two different chimpanzee MHC class I molecules, respectively [38-40]. The pairs of cross-reactive MHC presenting molecules differed by 6-42 residues, and had marked differences in the sequence and structure of the peptide binding groove. Yet, in all published cases, the peptide motifs of the cross-reactive MHC class I molecules were very similar. Our study presents a striking distinctiveness from the previous interspecies cross-reactivity reports, because the two presenting molecules, human HLA-Cw4 and mouse H-$2D^b$, that have up to 52 residue differences in the $\alpha_1\alpha_2$ peptide binding domains, have very different anchor motifs [30,31,33]. Thus, no similar anchor motifs are needed between interspecies cross-reactive MHC class I molecules to bind

very similar ligands. Finally, this finding shows the complexity and plasticity of interactions in MHC-peptide complexes.

In most cases, the natural MHC class I ligand is assumed to be the one that has the canonical anchor sites, the minimal length, and the optimal antigenicity when tested as a synthetic peptide. Two related studies of the endogenous processing of the HIV envelope glycoprotein would fence this hypothesis. The first study identified two peptide species of different lengths that share the same antigenic core associated with the D^d presenting molecule in infected cells [21]. These species were the optimal decapeptide and, unexpectedly, a nonamer that lacked the correctly positioned NH_3^+-terminal residue to bind the D^d molecule. Notably, both were equally antigenic for specific CTLs. Similarly, the second study involved the analysis of the same envelope glycoprotein and identified a nested set of three natural H-2L^d class I ligands of 15-, 10-, and 9-aa in length with identical C-terminal core [22]: the nonamer with the canonical anchor motif for binding to L^d and two additional unexpected species with either one or six N-terminally extended residues. Notably, the peptide with six N-terminally extended residues was ten-fold less antigenic but more abundant in infected cells than the core nine residues peptide. In line with these reports, our current study reveals that the natural octameric ligand obtained from HLA-Cw4$^+$ infected cells is not the optimal MHC class I binding peptide, as indicated by its lower *in vitro* affinity to HLA-Cw4 molecules compared with the nonamer that has one N-terminal additional residue. If assays with truncated overlapping synthetic peptides had been used, as is often the case in vaccine development, the nonamer but not the natural octamer would have been defined as the optimal HLA-Cw4 class I ligand. Thus, the extrapolation of either antigenicity or MHC binding strength is not sufficient to identify natural viral MHC class I ligands. These limitations may apply to the previous definition of the nonameric M187-195 peptide as a D^b-restricted CTL epitope [32]. In that study, the truncated overlapping synthetic peptides strategy was used. Both M187–195 and M188–195 peptides induced significant IFN-γ production by $CD8^+$ T cells, which was slightly higher for the

nonamer, in agreement with the D^b binding data shown in Figure 5. As the nonamer fits the canonical length for a MHC class I epitope and was predicted by every computer algorithm used, it was defined as the optimal epitope by the authors of the study [32]. The M188–195 peptide without an N-terminal residue would bind to H-$2D^b$ molecules as other peptides lacking the N-terminal binding residue do, as they have been endogenously identified bound to other MHC class I molecules [21,41], indicating that canonical MHC-peptide interactions in the P1 pocket are not always necessary for endogenous peptide presentation. Thus, only the detection of one or both peptides in the pool of D^b ligands in infected murine cells will determine the exact nature of the HRSV matrix epitope.

Collectively, the results in the current report highlight the importance of analyzing natural peptides that result from the endogenous processing of viral proteins. This analysis is fundamental for a detailed understanding of MHC class I-restricted immunity and future vaccine design.

METHODS

Cell Lines and Antibodies (Ab).

B27-C1R is a transfectant [42] of the human lymphoid cell line HMy2.C1R (C1R) with low expression of its endogenous class I molecules [28,29]. RMA-S is a TAP-deficient murine cell line [43]. The RMA-S transfectant cells expressing HLA-A2 [44], -B27 [45], -B35 [46], and -Cw4 [47] have been previously described. All cell lines were cultured in RPMI 1640 supplemented with 10% fetal bovine serum and $5x10^{-5}$ M β-mercaptoethanol. The Abs used in this study were the polyclonal FITC anti-HRSV, which recognizes HRSV F and G proteins (Chemicon International, Single Oak Drive Temecula, CA, USA), and the monoclonal Abs 34-5-8S (specific for H-2D^b) [48], W6/32 (specific for a monomorphic HLA-A, B, C determinant) [49], PA2.1 (specific for HLA-A2) [50], and ME1 (specific for HLA-B27, B7, Bw22) [51].

Synthetic Peptides.

Peptides were synthesized in a peptide synthesizer (model 433A; Applied Biosystems, Foster City, CA), and purified by reversed-phase HPLC. The monosubstituted Ala analogues of HRSV Matrix peptides were named according with the position of to the substituted residue (Ala → Ile or Ala → Thr) and their length. Thus, A2-8 refers to the octamer of sequence A<u>A</u>TNAKII. The correct molecular mass of peptides was established by MALDI-TOF MS, and the correct composition of HRSV peptides was determined with quadrupole ion trap microHPLC.

Isolation of HLA-bound peptides.

HLA-bound peptides were isolated from $2x10^9$ B27-C1R transfectant cells either infected or not infected with HRSV. Cells were lysed in 1% Igepal CA-630 (Sigma), 20

mM Tris/HCl buffer, 150 mM NaCl, pH 7.5, in the presence of a cocktail of protease inhibitors. HLA-peptide complexes were isolated by affinity chromatography of the soluble fraction with the W6/32 mAb. HLA-bound peptides were eluted at room temperature with 0.1% aqueous trifluoroacetic acid (TFA), concentrated with Centricon 3 (Amicon, Beberly, MA), and fractionated by high performance liquid chromatography (HPLC), as previously described [24,25].

Matrix-assisted laser desorption/ionization time-of-flight (MALDI-TOF) mass spectrometry.

HPLC fractions were analyzed using a MALDI-TOF mass spectrometer (Reflex IV, Bruker Daltoniks, Bremen, Germany). The samples were dried down with a SpeedVac system (Savant Global Medical Instrumentation, Ramsey,MN) and reconstituted in 1 µl of TA buffer (33% aqueous acetonitrile, 0.1% TFA). One fifth of the volume was loaded onto an MTP 384 massive 384-well MALDI insert (Bruker Daltoniks), and allowed to dry at room temperature. The remainder of each HPLC fraction was stored at 4ºC. Then, 0.6 µl of matrix solution (α-Cyano-4-hydroxycinnamic acid (Bruker Daltoniks) at 3 mg/ml was added to the MALDI insert and allowed to dry at room temperature. MS data were acquired in the mass range of 400-3000 Da in reflector positive mode at 25 kV and analyzed using the Flex Analysis software version 2.0 (Bruker Daltoniks). Each spectrum was externally calibrated with the Peptide Calibration Standard Mixture (Brucker Daltoniks, Product # 206195) to reach a typical mass measurement accuracy of <25 ppm.

Electrospray-ion trap mass spectrometry analysis.

Peptide sequencing was carried out by quadrupole ion trap electrospray MS/MS on a Deca XP LCQ instrument (Thermo Electron, San Jose, CA) coupled to microHPLC

(Biobasic C18 column 150x0.18 mm, Thermo Electron). The eluents used were the following: A, 0.5% acetic acid in water; and B, 80% acetonitrile containing 0.5% acetic acid. The gradient was 0-40% B in 24 min and 40-100% B in 5 min, with a flow rate of 1.5 µl/min. The MS/MS mode focused on each hypothetical parental peptide, previously selected by MALDI-TOF analysis and comparison, with an isolation width (m/z) of 1.5 Da was used [52]. The charge and the mass of the ionic species were determined by high-resolution sampling of the mass/charge rank. Collision energy and ion-precursor resolution were improved to optimize the fragmentation spectrum. MS spectra were processed using both Bioworks Browser (version 3.3.1 SP1) and Proteome Discovered 1.0 software (both from Thermo Electron) utilizing the National Center for Biotechnology Information non-redundant (NCBInr) protein database (July 2008 versions) within the taxonomy parameters of *Homo sapiens* and viruses. No enzyme specificity was selected. The peptide and MS/MS tolerances were set to ± 0.4 and ± 0.8 Da, respectively. In addition, the corresponding synthetic peptide was prepared, and its MS/MS spectrum was used to confirm the assigned sequence of the HRSV ligand.

MHC/Peptide Stability Assays.

The following synthetic peptides were used as controls in complex stability assays: KPNA2 (GLVPFLVSV, HLA-A2-restricted) [53], Flu NP (SRYWAIRTR, HLA-B27-restricted) [54], EBNA3 (YPLHEQHGM, HLA-B35-restricted) [55], and C4CON (QYDDAVYLK, HLA-Cw4-restricted) [56]. RMA-S transfectants were incubated at 26 °C for 16 h in RPMI 1640 medium supplemented with 10% heat-inactivated fetal bovine serum. Later, they were washed and incubated for 1 h at 26 °C with various peptide concentrations in medium without FCS, transferred to 37 °C, and collected for flow cytometry after 4 h. MHC expression was measured using 100 µl of hybridoma culture supernatant containing mAbs ME1 (anti-HLA-B27), PA2.1 (anti-HLA-A2), W6/32 (anti-

HLA monomorphic), or 34-5-8S (anti-H-2D^b) as described [57]. Samples were acquired on a FACSCanto flow cytometer (BD Biosciences, San Jose, CA, USA) and analyzed using CellQuest Pro 2.0 software (BD Bioscience). Cells incubated without peptide had peak fluorescence intensities close to background staining with secondary Ab alone. The fluorescence index was calculated at each time point as the ratio of mean channel fluorescence of the sample to that of the control incubated without peptide. Binding of HRSV matrix peptides was also expressed as C_{50}, which is the molar concentration of the peptide giving 50% of the maximum fluorescence obtained at the concentration range between 100 and 0.001 µM.

Molecular dynamics.

Starting structures. Native C4CON HLA-Cw4 binding peptide was taken from chains A, B and C 1qqd PDB file. HRSV M187-195 peptide bound to HLA-Cw4 model was build with MODELLER9v7 program using the PDB 1qqd file as template. HRSV M188-195 peptide was modelled by removal of the N-terminal Arg residue from the previous HRSV M187-195 peptide model. Protonation states of ionizable groups for the three system were calculated using H++ server (http://biophysics.cs.vt.edu/H++) [58 59]. The positions of hydrogen atoms, standard atomic charges and radii for all the atoms were assigned according to the ff03 force field [60]. The complexes were immersed in cubic boxes of TIP3P water molecules large enough to guarantee that the shortest distance between the solute and the edge of the box was larger than 13 Å [61]. Counter ions were also added to maintain electro neutrality. Three consecutive minimizations were performed: i) the first one involving only hydrogen atoms; ii) the second only the water molecules and ions; and iii) the entire system.

Simulation details. Starting minimized structures, prepared as stated before, were simulated in the NPT ensemble using Periodic Boundary Conditions and Particle Mesh Ewald to treat long-range electrostatic interactions. The systems were then heated and

equilibrated in two steps: i) 200 ps of MD heating the whole system from 100 K to 300 K, and ii) equilibration of the entire system during 1.0 ns at 300 K. The equilibrated structures were the starting points for the 10 ns MD simulations at constant temperature (300 K) and pressure (1 atm). SHAKE algorithm was used to keep bonds involving H atoms at their equilibrium length, allowing a 2 fs time step for the integration of Newton's equations of motion. ff03 and TIP3P force fields, as implemented in AMBER 10 package (http://ambermd.org/), were used to describe the proteins, the peptides, and the water molecules respectively. Sample frames at 20 ps intervals from the molecular dynamics trajectory were subsequently used for the analysis.

Interaction energies analysis. Effective binding free energies between the peptides and HLA-Cw4 were estimated using the MM-GBSA approach as implemented in the AMBER10 package [62]. MM-GBSA method approaches the free energy of binding as a sum of a molecular mechanics (MM) interaction term, a solvation contribution thorough a generalized Born (GB) model, and a surface area (SA) contribution to account for the non polar part of solvation. In addition, to better characterize peptides-protein interactions, an energy decomposition analysis in a pairwise fashion (between the peptides residues and HLA-Cw4 residues) was performed using a cut off of 5Å from the peptides. Polar contribution to solvation free energies were calculated with GB, whereas nonpolar were estimated to be proportional to the area lost upon binding using the LCPO method to calculate accessible surface areas [63]. These calculations were performed for each snapshot from the simulations using the appropriate module within AMBER 10 package.

ACKNOWLEDGEMENTS

We thank Drs. E. O. Long (National Institute of Allergy and Infectious Diseases, NIH, Rockville, MD, USA), M. Takiguchi (Center for AIDS Research, Kumamoto University, Kumamoto, Japan) and J. A. López de Castro (Centro de Biología Molecular Severo Ochoa, Madrid, Spain) for cell lines. We also thank Drs. A. Morreale and D. Abia (Centro de Biología Molecular Severo Ochoa, Madrid, Spain) for molecular modeling and the generous allocation of computer time at the Barcelona Supercomputing Center. This work was supported by grants from the Programa Ramón y Cajal, and Fondo de Investigaciones Sanitarias, to D. L., and from the Ministerio de Educación y Ciencia and Redes Temáticas de Investigación Cooperativa to M. D. V.

CONFLICT OF INTEREST

The authors declare that they have no competing financial interests

List of abbreviations:

APC, Antigen presenting cells

CTL, Cytotoxic T lymphocytes

ESI-IT, Electrospray ionization-Ion trap

HLA, Human histocompatibility complex

HRSV, Human Respiratory Syncytial Virus

LC-MS, Liquid chromatography-mass spectrometry

MALDI-TOF MS, Matrix-assisted laser desorption/ionization mass spectrometry

MHC, Major Histocompatibility Complex

MS/MS Tandem mass spectrometry

REFERENCES

1 Shastri N, Schwab S, Serwold T. Producing nature's gene-chips: the generation of peptides for display by MHC class I molecules. *Annu. Rev. Immunol.* 2002; **20:** 463-93.

2 Parker KC, Bednarek MA, Coligan JE. Scheme for ranking potential HLA-A2 binding peptides based on independent binding of individual peptide side-chains. *J. Immunol.* 1994; **152:** 163-75.

3 Rammensee HG, Bachmann J, Emmerich NPN, Bachor OA, Stevanovic S. SYFPEITHI: database for MHC ligands and peptide motifs. *Immunogenetics* 1999; **50:** 213-9.

4 Bjorkman PJ, Saper MA, Samraoui B, Bennett WS, Strominger JL, Wiley DC. Structure of the human class I histocompatibility antigen, HLA-A2. *Nature* 1987; **329:** 506-12.

5 Bjorkman PJ, Saper MA, Samraoui B, Bennett WS, Strominger JL, Wiley DC. The foreign antigen binding site and T cell recognition regions of class I histocompatibility antigens. *Nature* 1987; **329:** 512-8.

6 York IA, Goldberg AL, Mo XY, Rock KL. Proteolysis and class I major histocompatibility complex antigen presentation. *Immunol. Rev.* 1999; **172:** 49-66.

7 Collins PL, Chanock RM, Murphy BR. Respiratory Syncytial Virus. In: Lippincott Williams & Wilkins (ed.) *Fields Virology*. 2007; 1443-1486.

8 Hall CB. Respiratory syncytial virus and parainfluenza virus. *N. Engl. J. Med.* 2001; **344:** 1917-28.

9 Shay DK, Holman RC, Roosevelt GE, Clarke MJ, Anderson LJ. Bronchiolitis-associated mortality and estimates of respiratory syncytial virus-associated deaths among US children, 1979-1997. *J. Infect. Dis.* 2001; **183:** 16-22.

10 Thompson WW, Shay DK, Weintraub E *et al.* Mortality associated with influenza and respiratory syncytial virus in the United States. *JAMA* 2003; **289:** 179-86.

11 Wendt CH, Hertz MI. Respiratory syncytial virus and parainfluenza virus infections in the immunocompromised host. *Semin. Respir. Infect.* 1995; **10:** 224-31.

12 Ison MG, Hayden FG. Viral infections in immunocompromised patients: what's new with respiratory viruses? *Curr. Opin. Infect. Dis.* 2002; **15:** 355-67.

13 Han LL, Alexander JP, Anderson LJ. Respiratory syncytial virus pneumonia among the elderly: an assessment of disease burden. *J Infect. Dis* 1999; **179:** 25-30.

14 Falsey AR, Hennessey PA, Formica MA, Cox C, Walsh EE. Respiratory syncytial virus infection in elderly and high-risk adults. *N. Engl. J. Med.* 2005; **352:** 1749-59.

15 Anderson LJ, Heilman CA. Protective and disease-enhancing immune responses to respiratory syncytial virus. *J Infect. Dis.* 1995; **171:** 1-7.

16 Brandenburg AH, de Waal L, Timmerman HH, Hoogerhout P, de Swart RL, Osterhaus AD. HLA class I-restricted cytotoxic T-cell epitopes of the respiratory syncytial virus fusion protein. *J Virol* 2000; **74:** 10240-4.

17 Rock MT, Crowe JE. Identification of a novel human leucocyte antigen-A*01-restricted cytotoxic T-lymphocyte epitope in the respiratory syncytial virus fusion protein. *Immunology* 2003; **108:** 474-80.

18 Venter M, Rock M, Puren AJ, Tiemessen CT, Crowe JE, Jr. Respiratory syncytial virus nucleoprotein-specific cytotoxic T-cell epitopes in a South African population of diverse HLA types are conserved in circulating field strains. *J. Virol.* 2003; **77:** 7319-29.

19 Heidema J, de Bree GJ, De Graaff PM *et al.* Human CD8(+) T cell responses against five newly identified respiratory syncytial virus-derived epitopes. *J. Gen. Virol.* 2004; **85:** 2365-74.

20 Terrosi C, Di Genova G, Savellini GG, Correale P, Blardi P, Cusi MG. Immunological characterization of respiratory syncytial virus N protein epitopes recognized by human cytotoxic T lymphocytes. *Viral Immunol.* 2007; **20:** 399-406.

21 Samino Y, López D, Guil S, de León P, Del Val M. An endogenous HIV envelope-derived peptide without the terminal NH_3+ group is physiologically presented by major histocompatibility class I molecules. *J. Biol. Chem.* 2004; **279:** 1151-60.

22 Samino Y, López D, Guil S, Saveanu L, van Endert PM, Del Val M. A long N-terminal-extended nested set of abundant and antigenic major histocompatibility complex class I natural ligands from HIV envelope protein. *J. Biol. Chem.* 2006; **281:** 6358-65.

23 Meiring HD, Soethout EC, Poelen MC *et al.* Stable isotope tagging of epitopes: a highly selective strategy for the identification of major

histocompatibility complex class I-associated peptides induced upon viral infection. *Mol. Cell Proteomics.* 2006; **5:** 902-13.

24 Cragnolini JJ, Lopez de Castro JA. Identification of endogenously presented peptides from Chlamydia trachomatis with high homology to human proteins and to a natural self-ligand of HLA-B27. *Mol. Cell Proteomics.* 2008; **7:** 170-80.

25 Cragnolini JJ, Garcia-Medel N, Lopez de Castro JA. Endogenous processing and presentation of T-cell Epitopes from chlamydia trachomatis with relevance in HLA-B27-associated reactive arthritis. *Mol. Cell Proteomics.* 2009; **8:** 1850-9.

26 Bangham CR, McMichael AJ. Specific human cytotoxic T cells recognize B-cell lines persistently infected with respiratory syncytial virus. *Proc. Natl. Acad. Sci. U. S. A.* 1986; **83:** 9183-7.

27 Lopez de Castro JA, Alvarez I, Marcilla M *et al.* HLA-B27: a registry of constitutive peptide ligands. *Tissue Antigens* 2004; **63:** 424-45.

28 Storkus WJ, Howell DN, Salter RD, Dawson JR, Cresswell P. NK susceptibility varies inversely with target cell class I HLA antigen expression. *J. Immunol.* 1987; **138:** 1657-9.

29 Zemmour J, Little AM, Schendel DJ, Parham P. The HLA-A,B "negative" mutant cell line C1R expresses a novel HLA-B35 allele, which also has a point mutation in the translation initiation codon. *J Immunol.* 1992; **148:** 1941-8.

30 Falk K, Rotzschke O, Grahovac B *et al.* Allele-specific peptide ligand motifs of HLA-C molecules. *Proc. Natl Acad. Sci U. S. A* 1993; **90:** 12005-9.

31 Buchsbaum S, Barnea E, Dassau L, Beer I, Milner E, Admon A. Large-scale analysis of HLA peptides presented by HLA-Cw4. *Immunogenetics* 2003; **55:** 172-6.

32 Rutigliano JA, Rock MT, Johnson AK, Crowe JE, Jr., Graham BS. Identification of an H-2D(b)-restricted CD8+ cytotoxic T lymphocyte epitope in the matrix protein of respiratory syncytial virus. *Virology* 2005; **337:** 335-43.

33 Falk K, Rotzschke O, Stevanovic S, Jung G, Rammensee HG. Allele-specific motifs revealed by sequencing of self-peptides eluted from MHC molecules. *Nature* 1991; **351:** 290-6.

34 Fan QR, Wiley DC. Structure of human histocompatibility leukocyte antigen (HLA)-Cw4, a ligand for the KIR2D natural killer cell inhibitory receptor. *J Exp. Med* 1999; **190:** 113-23.

35 Garcia AM, Ortiz-Navarrete VF, Mora-Garcia ML *et al.* Identification of peptides presented by HLA class I molecules on cervical cancer cells with HPV-18 infection. *Immunol. Lett.* 1999; **67:** 167-77.

36 Johnson RP, Trocha A, Buchanan TM, Walker BD. Recognition of a highly conserved region of human immunodeficiency virus type 1 gp120 by an HLA-Cw4-restricted cytotoxic T-lymphocyte clone. *J Virol.* 1993; **67:** 438-45.

37 Stratov I, Dale CJ, Chea S, McCluskey J, Kent SJ. Induction of T-cell immunity to antiretroviral drug-resistant human immunodeficiency virus type 1. *J Virol* 2005; **79:** 7728-37.

38 Hickman-Miller HD, Bardet W, Gilb A *et al.* Rhesus macaque MHC class I molecules present HLA-B-like peptides. *J Immunol.* 2005; **175:** 367-75.

39 Sette A, Sidney J, Bui HH *et al.* Characterization of the peptide-binding specificity of Mamu-A*11 results in the identification of SIV-derived epitopes and interspecies cross-reactivity. *Immunogenetics* 2005; **57:** 53-68.

40 Cooper S, Kowalski H, Erickson AL *et al.* The presentation of a hepatitis C viral peptide by distinct major histocompatibility complex class I allotypes from two chimpanzee species. *J Exp. Med* 1996; **183:** 663-8.

41 Yagüe J, Marina A, Vázquez J, López de Castro JA. Major histocompatibility complex class I molecules bind natural peptide ligands lacking the amino-terminal binding residue in vivo. *J. Biol. Chem.* 2001; **276:** 43699-707.

42 Calvo V, Rojo S, Lopez D, Galocha B, Lopez dCJ. Structure and diversity of HLA-B27-specific T cell epitopes. Analysis with site-directed mutants mimicking HLA-B27 subtype polymorphism. *J. Immunol.* 1990; **144:** 4038-45.

43 Ljunggren HG, Karre K. Host resistance directed selectively against H-2-deficient lymphoma variants. Analysis of the mechanism. *J. Exp. Med.* 1985; **162:** 1745-59.

44 Anderson KS, Alexander J, Wei M, Cresswell P. Intracellular transport of class I MHC molecules in antigen processing mutant cell lines. *J Immunol.* 1993; **151:** 3407-19.

45 Villadangos JA, Galocha B, Lopez de Castro JA. Unusual topology of an HLA-B27 allospecific T cell epitope lacking peptide specificity. *J. Immunol.* 1994; **152:** 2317-23.

46 Kubo H, Ikeda-Moore Y, Kikuchi A *et al.* Residue 116 determines the C-terminal anchor residue of HLA- B*3501 and -B*5101 binding peptides but does not explain the general affinity difference. *Immunogenetics* 1998; **47:** 256-63.

47 Rajagopalan S, Long EO. The direct binding of a P58 killer cell inhibitory receptor to Human Histocompatibility leukocyte antigen (HLA)-CW4 exhibits peptide selectivity. *Journal of Experimental Medicine* 1997; **185:** 1523-8.

48 Ozato K, Mayer NM, Sachs DH. Monoclonal antibodies to mouse major histocompatibility complex antigens. *Transplantation* 1982; **34:** 113-20.

49 Barnstable CJ, Bodmer WF, Brown G *et al.* Production of monoclonal antibodies to group A erythrocytes, HLA and other human cell surface antigens-new tools for genetic analysis. *Cell* 1978; **14:** 9-20.

50 Parham P, Bodmer WF. Monoclonal antibody to a human histocompatibility alloantigen, HLA-A2. *Nature* 1978; **276:** 397-9.

51 Ellis SA, Taylor C, McMichael A. Recognition of HLA-B27 and related antigen by a monoclonal antibody. *Hum. Immunol.* 1982; **5:** 49-59.

52 López D, Calero O, Jiménez M, García-Calvo M, Del Val M. Antigen processing of a short viral antigen by proteasomes. *J. Biol. Chem.* 2006; **281:** 30315-8.

53 Hunt DF, Henderson RA, Shabanowitz J *et al.* Characterization of peptides bound to the class I MHC molecule HLA-A2.1 by mass spectrometry. *Science* 1992; **255:** 1261-3.

54 Wang M, Lamberth K, Harndahl M *et al.* CTL epitopes for influenza A including the H5N1 bird flu; genome-, pathogen-, and HLA-wide screening. *Vaccine* 2007; **25:** 2823-31.

55 Burrows SR, Gardner J, Khanna R *et al.* Five new cytotoxic T cell epitopes identified within Epstein-Barr virus nuclear antigen 3. *J Gen Virol* 1994; **75 (Pt 9):** 2489-93.

56 Fan QR, Garboczi DN, Winter CC, Wagtmann N, Long EO, Wiley DC. Direct binding of a soluble natural killer cell inhibitory receptor to a soluble human leukocyte antigen-CW4 class I Major Histocompatibility Complex molecule. *Proc. Natl. Acad. Sci. U. S. A.* 1996; **93:** 7178-83.

57 López D, Samino Y, Koszinowski UH, Del Val M. HIV envelope protein inhibits MHC class I presentation of a cytomegalovirus protective epitope. *J. Immunol.* 2001; **167:** 4238-44.

58 Gordon JC, Myers JB, Folta T, Shoja V, Heath LS, Onufriev A. H++: a server for estimating pKas and adding missing hydrogens to macromolecules. *Nucleic Acids Res* 2005; **33:** W368-W371.

59 Anandakrishnan R, Onufriev A. Analysis of basic clustering algorithms for numerical estimation of statistical averages in biomolecules. *J Comput. Biol.* 2008; **15:** 165-84.

60 Duan Y, Wu C, Chowdhury S *et al.* A point-charge force field for molecular mechanics simulations of proteins based on condensed-phase quantum mechanical calculations. *J Comput. Chem.* 2003; **24:** 1999-2012.

61 Jorgensen WL, Chandrasekhar J, Madura JD, Impey RW, Klein ML. Comparison of simple potential functions for simulating liquid water. *J. Chem. Phys.* 1983; **79:** 926-35.

62 Still W, Clark, Tempczyk A, Hawley RC, Hendrickson TY. Semianalytical treatment of solvation for molecular mechanics and dynamics. *J. Am. Chem. Soc.* 1990; **112:** 6127-9.

63 Weiser J, Shenkin PS, Still WC. Approximate atomic surfaces from linear combinations of pairwise overlaps (LCPO). *J. Com. Chem.* 2009; **20:** 217-30.

FIGURES

Figure 1. Persistent infection of the B27-C1R cell line by HRSV.

The B27-C1R cell line was infected with Long strain of HRSV at a MOI of 2 PFU/cell, incubated for 2 h at 37ºC and then washed. A mock infected control was included as negative control. The cells were then cultured for 2 weeks and stained with the polyclonal FITC-labelled anti-HRSV Ab that recognizes HRSV F and G proteins. Samples were analyzed by FACS (B27-C1R mock infected, upper panel; and HRSV-infected B27-C1R cells, lower panel).

Figure 2. Identification of the M188-195 ligand in infected cell extracts by mass spectrometry.

The MS/MS fragmentation spectrum was obtained after quadrupole ion trap mass spectrometry of the ion peak at *m/z* 422.9 of the extract of B27-C1R cells infected with HRSV (upper panel) and the corresponding synthetic peptide (lower panel). The vertical axis represents the relative abundance of the parental ion and each fragmentation ion detected. Ions generated in the fragmentation are detailed, while the sequence deduced from the indicated fragments is shown in the upper left box of each respective panel.

Figure 3. HLA stabilization assay with HRSV M188-195 synthetic peptidic ligand.

Stability at the cell surface of HLA-B27 (panel a), -A2 (panel b), or –B35 (panel c), of RMA-S cells transfected with each of these HLA class I molecules, respectively, was measured by flow cytometry. The indicated peptides were used at 200 µM. The mAbs used were ME1 (anti-HLA-B27, panel a), PA2.1 (anti-HLA-A2, panel b), W6/32 (anti-

HLA monomorphic, panel c). The results, calculated as FI (see "Materials and Methods") ± SD, are the mean of 2-4 independent experiments.

Figure 4. HLA stabilization assay with HRSV M188-195 and M187-195 synthetic peptides.

Stability at the cell surface of HLA-Cw4 (upper left panel), or H-2D^b (upper right panel) of the respective RMA-S transfectant cells was measured by flow cytometry. The indicated peptides were used at 200 µM. The mAbs used were W6/32 (anti-HLA monomorphic , left panel) and 34-5-8S (anti-H-2D^b, right panel). A representative experiment with HLA-Cw4 RMA-S cells was depicted in the bottom panel. The coded used as in follows: isotypic control (shaded histogram), C4CON peptide (thick line), and M188-195 peptide (thin line). The data, calculated as in Figure 3, are the mean of 2-5 independent experiments.

Figure 5. Binding affinity to MHC of HRSV M188-195 and M187-195 synthetic peptides.

Synthetic peptides HRSV M188-195 (squares), M187-195 (circles), and Flu NP (negative control, triangles) were titrated on cells expressing HLA-Cw4 (left panel) or H-2D^b (right panel) and stabilization of MHC was measured by flow cytometry. The data, calculated as in Figures 3 and 4, are the mean of 3-5 independent experiments. The calculated C_{50} values (see "Materials and Methods") ± SD are shown below.

Figure 6. Modeling of HLA-Cw4-bound conformations of peptides C4CON (QYDDAVYKL), HRSV M188-195 (NAITNAKII) and M187-195 (AITNAKII).

Backbone atoms of the indicated HLA-Cw4-bound peptides are displayed as ribbon tubes (Panel a, QYDDAVYKL; panel b, NAITNAKII; and panel c: AITNAKII). Atoms are represented by sticks with the following colour scheme: blue, nitrogen; red, oxygen; green, carbon atom. The peptide residues that interact with the HLA-Cw4 pockets are indicated. The HLA-Cw4 protein is not displayed. The figure was prepared using the PyMOL program.

Figure 7. HLA stabilization assay with monosubstituted Ala analogues of HRSV M188-195 and M187-195 synthetic peptides.

Stability at the cell surface of HLA-Cw4 RMA-S transfectant cells was measured by flow cytometry. The indicated peptides were used at 200 µM. The mAb used was W6/32 (anti-HLA monomorphic). The data, calculated as in Figure 3, are the mean of 3 independent experiments.

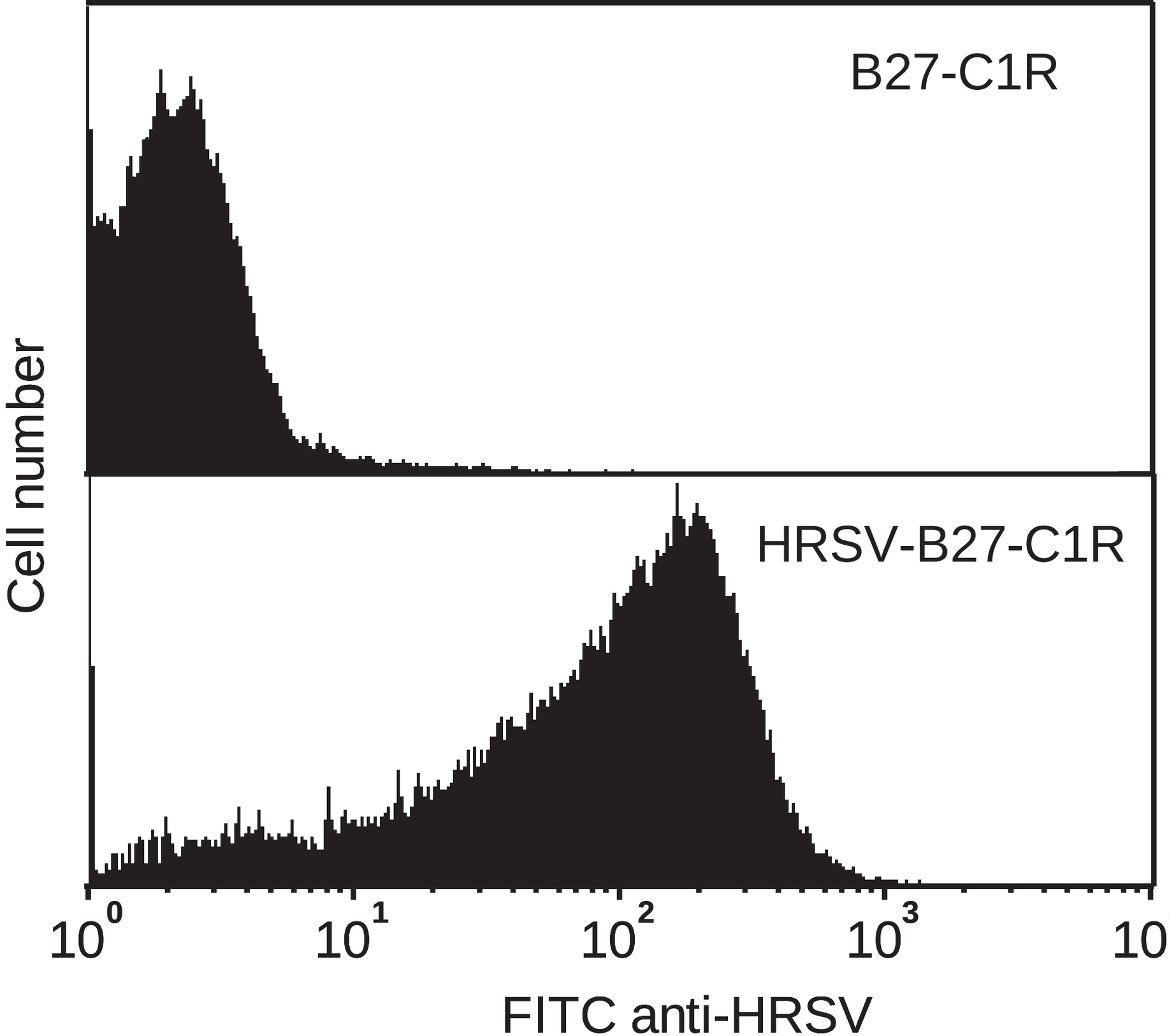

Infantes et al. Figure 1

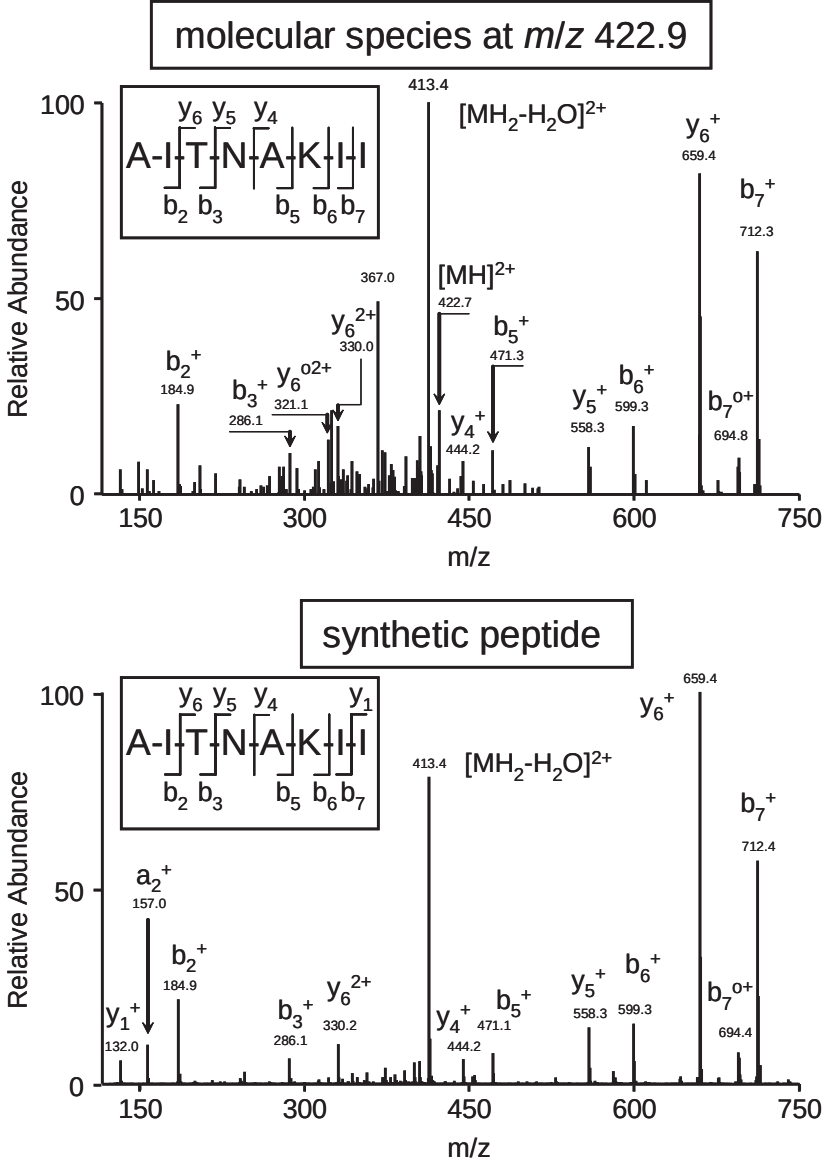

Infantes et al. Figure 2

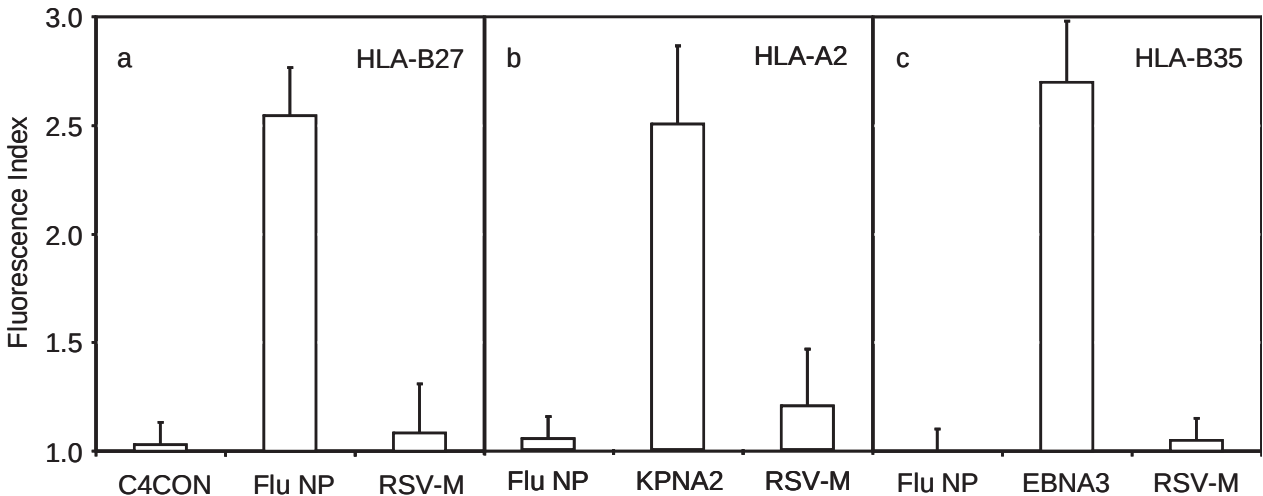

Infantes et al. Figure 3

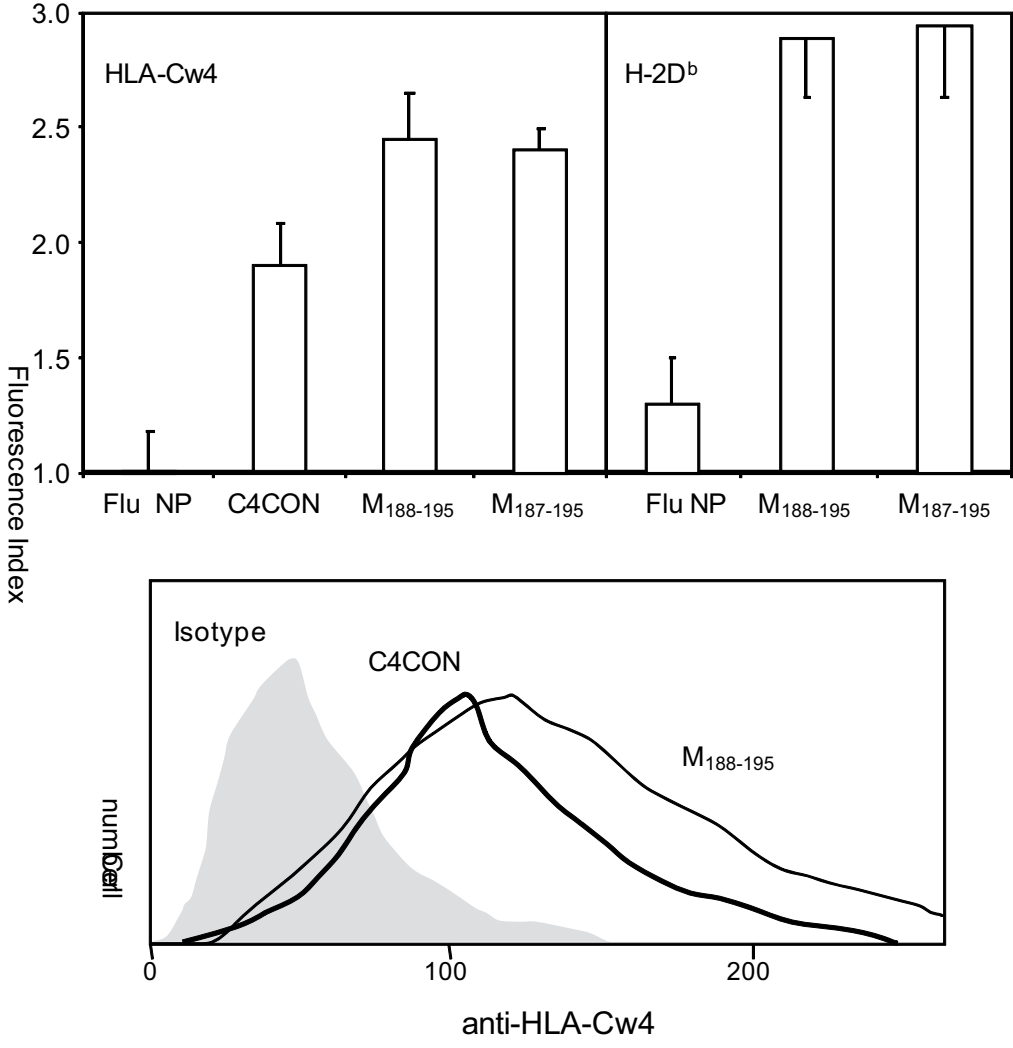

Infantes et al. Figure 4

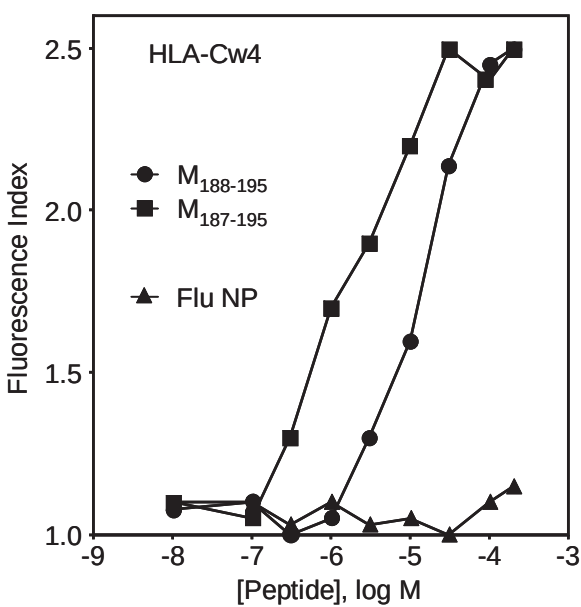

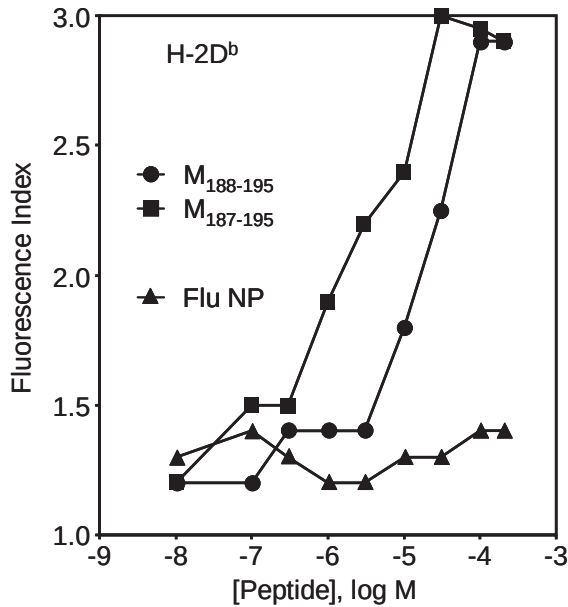

	C_{50} (μM)	
Peptide	HLA-Cw4	H-2D^b
RSV $M_{188-195}$	16 ± 12	22 ± 8
RSV $M_{187-195}$	1.5 ± 1	2 ± 1

Infantes et al. Figure 5

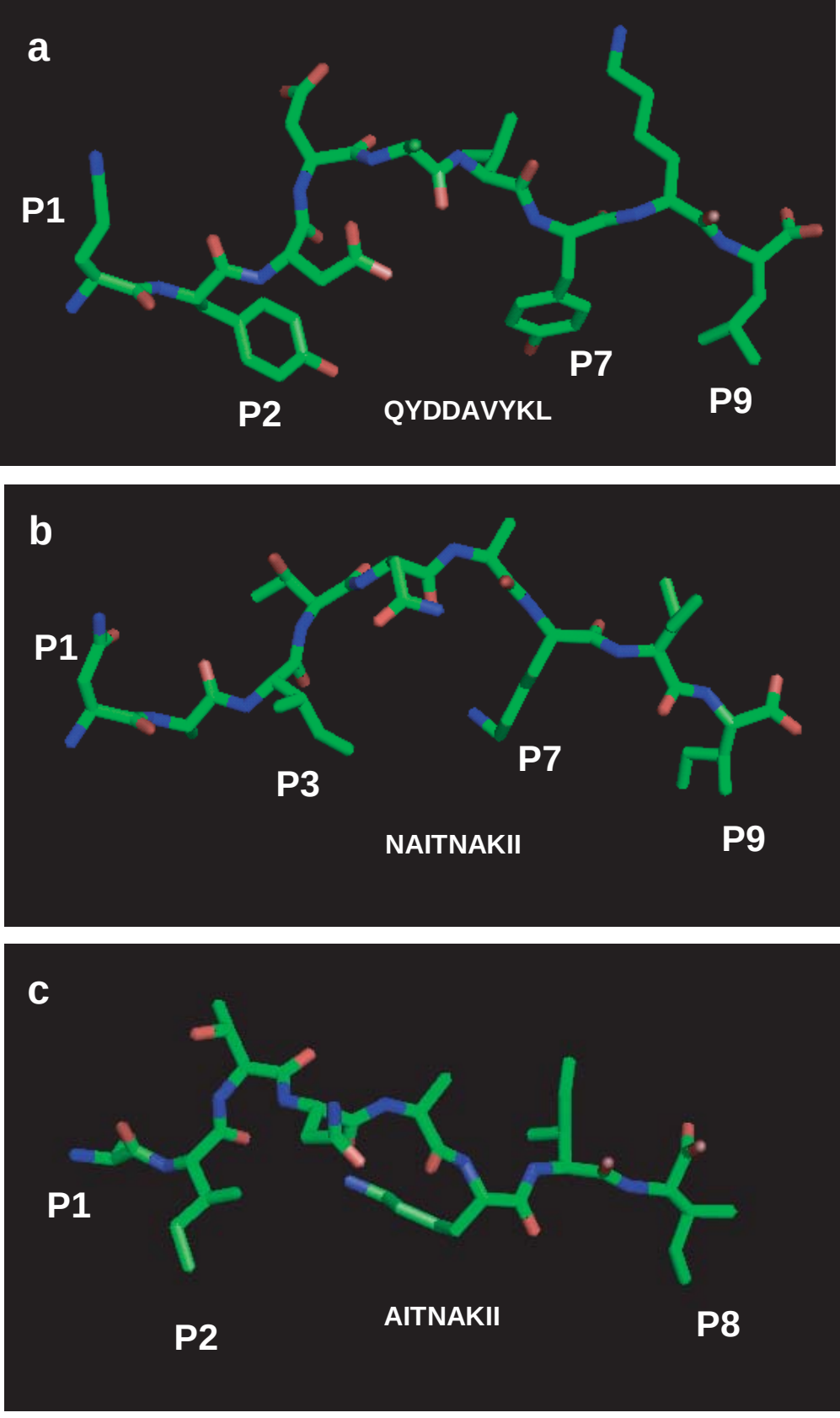

Infantes et al. Figure 6

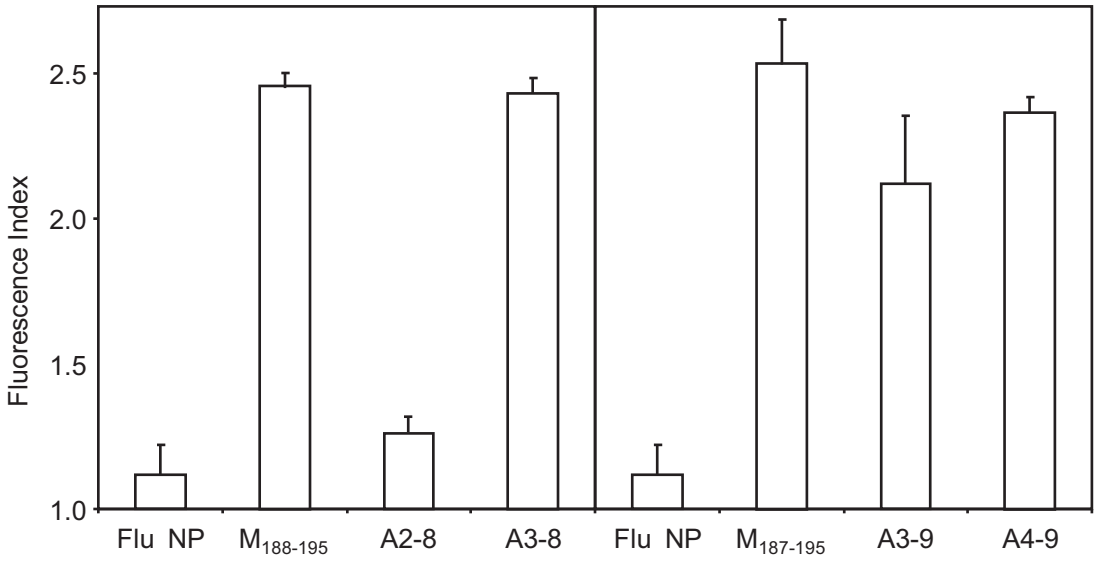

Infantes et al. Figure 7